Separation of heavy metal and protein from wastewater by sulfonated polyphenylsulfone ultrafiltration membrane process prepared by glycine betaine enriched coagulation bath

Irfana Moideen Kolangare*, Arun Mohan Isloor*,†, Asif Ali Qaiser**, Ahmed Fauzi Ismail***,
and Mohd Sohaimi Abdullah***

*Membrane Technology Laboratory, Department of Chemistry, National Institute of Technology Karnataka,
Surathkal, Mangalore-575 025, India
**Department of Polymer and Process Engineering, University of Engineering and Technology Lahore,
54890, Lahore, Pakistan
***Advanced Membrane Technology Research Center (AMTEC), Universiti Teknologi Malaysia,
81310 Skudai, Johor Bahru, Malaysia

Abstract−This work deals with a simple and eco-friendly approach for the development of ultrafiltration membranes for the separation of environmentally hazardous substances from the water source. Polysulfone and sulfonated polyphenylsulfone blend ultrafiltration membranes were fabricated by the non-solvent induced phase inversion technique. Prepared membranes were characterized for their morphology, hydrophilicity, porosity, filtration and antifouling properties. The blend membranes with 15 wt% of sPPSU demonstrated the best performance with water flux of 190.33 $Lm^{-2}h^{-1}$ and flux recovery ratio of 86.56%. The effect of aq. glycine betaine (GB) coagulation bath on the membrane property and performance was studied and compared with commonly used additives such as NaCl and NMP. The GB in coagulation bath exhibited better flux and performance with protein rejection of 66.3%, 74.0% and 91.2% for trypsin, pepsin, and bovine serum albumin, respectively, and heavy metal rejection of 75.2% and 87.6% for polymer enhanced ultrafiltration of Cd^{2+} and Pb^{2+} ions, respectively.

Keywords: Sulfonated Polyphenylsulfone, Glycine Betaine, Coagulation Bath, Protein Rejection, Heavy Metal Rejection

INTRODUCTION

Rapid industrial development and urbanization has led to the contamination of water resources due to the uncontrolled and unscientific disposal of hazardous waste into the water bodies. These non-biodegradable wastes such as heavy metals result in acute health and environmental issues due to bioaccumulation. Additionally, the carcinogenic nature of the heavy metals makes their removal from the water bodies a primary concern [1,2]. Proteins, on the other hand, cause biocontamination of water and make it unfit for potable use [3]. Moreover, the demand for protein removal and separation is increasing in food and pharmaceutical industries as the purified proteins are extremely valuable reagent in the biochemical and bio-organic applications [4,5].

Ultrafiltration (UF) membranes with high efficiency of separation, low operational cost, and mild operating conditions have made them a potential candidate for pretreatment of water by removal of proteins, chemicals, and toxic metals [3,6]. The UF process removes the solutes such as heavy metals and proteins based on their size and molecular weight by sieving mechanism [7,8]. The polyarylsulfone based polymers are commonly used membrane materials

due to their excellent mechanical strength with increased chemical and thermal resistance. However, their poor hydrophilicity is a major drawback which leads to membrane fouling, which is one among the chief issues affecting the performance, life, and reusability of the membrane [9]. However, functionalization of the aromatic structure of polymeric backbone with ionomeric groups, like sulfonic acid, carboxylic acid, amine etc. has been reported to improve its hydrophilicity [10-12].

The composition of casting solution and coagulation bath has reportedly been shown to affect the morphology and performance of the membrane. Asymmetric membranes are formed as a result of phase separation that takes place at a controlled rate, where the solvent and non-solvent interact to form the membrane with desired characteristics [13,14]. The coagulation bath composition can control the sub-layer formation of the membranes and bring changes in asymmetric structure [14-16]. Chun et al., reported that, the addition of dimethylacetamide (DMAC) in the coagulation bath delayed the liquid-liquid demixing during the phase inversion, which reduced the porosity and the pore size of the skin layers [17]. Yang and Liu also demonstrated the effect of salts like NaCl and Na_2CO_3 in the coagulation bath. They found increased membrane permeability with an increase in the concentration of Na_2CO_3 in the coagulant, while the permeability decreased with increased concentration of NaCl [18]. Yam-Cervantes et al. fabricated asymmetric sPPSU membrane using different coagulation bath composition

†To whom correspondence should be addressed.
E-mail: isloor@yahoo.com

such as acetone/IPA, and AA-NaHCO₃/IPA [19]. The AA-NaH-CO₃/IPA bath showed better morphology with spongy asymmetric structure due to a lower isoelectric point of the solvents when compared with AC/IPA coagulation bath, where finger-like structure is observed. NMP functioned as retardant when added to the coagulation bath as it avoids macrovoid formation. Therefore, incorporation of an additive such as solvents, inorganic salts or polymer to the coagulation bath can influence the mass transfer and the rate of liquid-liquid demixing [20,21].

The use of various additives such as NaCl, Na₂CO₃, NaOH, ethanol, methanol, glacial acetic acid, DMF, and NMP in coagulation bath has been reported in the literature [18,21,22]; however, the effect of zwitterionic glycine betaine (GB) on coagulation bath has not yet been studied. GB is a zwitterionic molecule which contains a cationic quaternary ammonium group and an anionic carboxylate group. It is a non-toxic osmolyte which is abundantly available both naturally and synthetically. It is also known to prevent protein aggregation and fouling interfaces as the trimethylglycine prevents the nonspecific protein adsorption [23]. The ability of GB to retain water makes it an ideal additive to improve the hydrophilicity of the membrane. Moreover, the incorporation additive in coagulation bath could overrule the drawbacks such as leaching, agglomeration of additives when added to the dope solution.

In current work, we developed polysulfone (PSF)/sulfonated polyphenylsulfone (sPPSU) blend ultrafiltration membranes with superior hydrophilicity and antifouling property for the removal of protein and heavy metal. The effect of the composition of sPPSU on morphology, hydrophilicity, hydraulic permeability and anti-fouling property of the prepared membranes was analyzed by scanning electron microscopy, contact angle measurement, and dead-end filtration experiments. The effect of GB in coagulation bath compositions on the membrane performances was also studied and compared with commonly used additives such as NaCl and NMP.

EXPERIMENTAL

1. Materials Used

PSF (Mw~35,000), GB (Mw~117.15), Cadmium nitrate tetrahydrate and lead nitrate were procured from Sigma-Aldrich Co., India. PPSU (Radel R-5000) (average Mw~50,000 g mol⁻¹) was purchased from Solvay Advanced Polymer (Belgium). NMP and conc. H₂SO₄ were from Merck India, Ltd. Bovine Serum Albumin (BSA) (Mw~67 kDa), Pepsin (Mw~35 kDa) and Trypsin (Mw~23 kDa) were from CDH Chemicals, India. NaCl was from Nice chemicals (P), Ltd. Polyethyleneimine (Mn~60,000) 50 wt% aq. Solution (branched) was from Acros Organics, USA.

2. Synthesis of sPPSU

PPSU (5 g) was dissolved in Conc. H₂SO₄ (500 mL) at 50 °C for five days under a nitrogen atmosphere (Scheme 1). The reaction mixture was then precipitated using a large volume of distilled ice-cold water with constant stirring. The white precipitate obtained was left overnight. It was filtered and washed with distilled ice-cold water to attain neutral pH. The sPPSU was dried under vacuum for 4-6 h at room temperature [24]. The polymer was characterized using ATR-FTIR and ¹H-NMR. The degree of sulfonation (DS) of
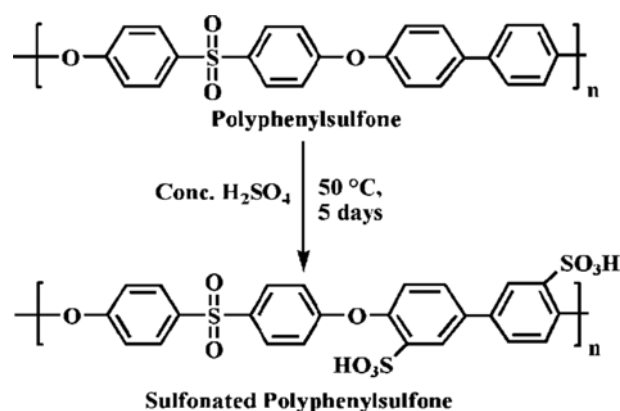
Scheme 1. Scheme for the sulfonation of PPSU.

Table 1. Compositions of dope solution and coagulation bath

Membrane code	Compositions (wt%)		
	Casting solution (20)		Coagulation bath
	PSF (%)	sPPSU (%)	
W 5	95	5	Distilled water
W 10	90	10	Distilled water
W 15	85	15	Distilled water
G 15	85	15	5% aq. GB
N 15	85	15	5% aq. NMP
S 15	85	15	5% aq. NaCl

the prepared polymer was determined by titration [25,26] and was found to be 37.2±2.3%.

$$DS = \frac{0.388 \times C_{NaOH} \times V_{NaOH}}{W - 0.081(C_{NaOH} \times V_{NaOH})} \qquad (1)$$

where 'W' is the weight of the sample, 'C_{NaOH}' is the concentration of the standard NaOH solution, 'V_{NaOH}' is the amount of NaOH solution consumed, 388 is the molecular weight of the repeating unit of PPSU, and 81 is the molecular weight of the -SO₃H segment.

3. Membrane Preparation

The casting solutions composition in NMP (80 wt%) is given in Table 1. Homogeneous solutions were obtained by stirring the blend at 60 °C for 24 h. The polymer solution was filtered and degassed for 15 min in an ultrasonic bath (40 kHz). The dope solution was cast onto a glass plate with a doctor's blade and dipped into a coagulation bath of different composition for phase inversion [27]. The membranes were then stored and characterized.

4. Membrane Characterization

The cross-sectional images of prepared membranes were obtained by scanning electron microscopy (SEM) (JEOL JSM-6380L). The membranes samples were prepared by freeze fracturing, i.e., the membrane sample was frozen in liquid nitrogen and broken apart to obtain the internal structure of the membrane. The fractured area of the sample was then sputter coated with gold to get the block face for the SEM [28].

The membrane surface topography was measured using atomic force microscopy (AFM). The AFM (Atomic force microscope)

device used was an Innova SPM Atomic Force Microscope with antimony doped silicon cantilever having a force constant in the range of 20-80 N/m. The membrane samples were dried and set on a substrate where the surface image was taken in tapping mode. The surface roughness parameters of the membranes were calculated including, average roughness (R_a) and root mean square roughness (R_q) [29].

The water contact angle (WCA) of the membranes was assessed using FTA-200 dynamic contact angle analyzer by sessile droplet method to analyze the membrane hydrophilicity. The average value was reported by measuring the water contact angle of membrane samples at three different sites [30].

The gravimetric method was used to study the water uptake capacity and porosity of the membranes [31]. The membrane samples of area $1 cm^2$ were dipped in the distilled water for 24 h. The membrane samples were weighed to obtain the wet weight after removing the excess water present on the membrane surface. It was then desiccated in a vacuum oven for 24 h, and the dry membrane samples were weighed. The wet and dry weight were used to calculate the water uptake and porosity of the membranes using the following equation,

$$\% \text{ water uptake} = \left(\frac{W_w - W_d}{W_d}\right) \times 100 \tag{2}$$

$$\varepsilon\,(\%) = \left(\frac{W_w - W_d}{Al\rho}\right) \times 100 \tag{3}$$

where 'W_w' and 'W_d' are the wet and dry weight of membrane, respectively, 'A' is the area of the sample (cm^2), 'l' is the membrane thickness (cm), and 'ρ' is the density of water ($0.998\,gcm^{-3}$).

The mean pore radius was determined by the filtration velocity method using Guerout-Elford-Ferry equation [32,33]:

$$r_m = \sqrt{\frac{(2.9 - 1.75\varepsilon) \times 8\eta lQ}{\varepsilon \times A \times \Delta P}} \tag{4}$$

where 'η' is the viscosity of water, 'Q' is the volume of permeate water per-unit time, and 'ΔP' is the operational membrane pressure.

5. Filtration and Antifouling Study

The pure water flux (PWF) and rejection (R) ability of the prepared membranes were evaluated by dead-end filtration at 0.3 MPa transmembrane pressure (TMP) as per Eqs. (5) and (6), respectively. The PWF and protein flux of the membrane with an effective membrane area of $25\,cm^2$ were measured by passing deionized water and protein solution separately as feed through the membranes [34].

The protein and complexed metal ion rejection studies were carried out by separately passing a protein solution of BSA, pepsin, and trypsin; and polyethyleneimine (PEI) complexed heavy metal (Pb^{+2}, Cd^{+2}) solution through the membranes respectively. The permeate collected was analyzed for protein rejection using a UV-Vis spectrophotometer at a wavelength of 280 nm and heavy metal using atomic absorption spectrophotometer (GBC 932 Plus).

$$J_{w1} = \frac{V}{\Delta t \times A} \tag{5}$$

$$R = \left(1 - \frac{C_p}{C_f}\right) \times 100 \tag{6}$$

where, 'J_{w1}' is PWF expressed in $Lm^{-2}h^{-1}$, 'V' (L) is volume of water passing through an effective membrane area 'A' (m^2) at time 'Δt' (h). 'C_p' and 'C_f' (mgL^{-1}) are the concentration of the solute in the permeate and feed, respectively.

The antifouling study was conducted by passing BSA solution (1,000 ppm) for 80 min and the flux of BSA solution (J_p) was measured using Eq. (5). After BSA filtration, the membranes were washed and then the PWF 'J_{w2}' ($Lm^{-2}h^{-1}$) of membrane was assessed again. The membrane fouling property was determined by flux recovery ratio (FRR), reversible (R_{rev}) and irreversible (R_{irr}) fouling ratio by following equations.

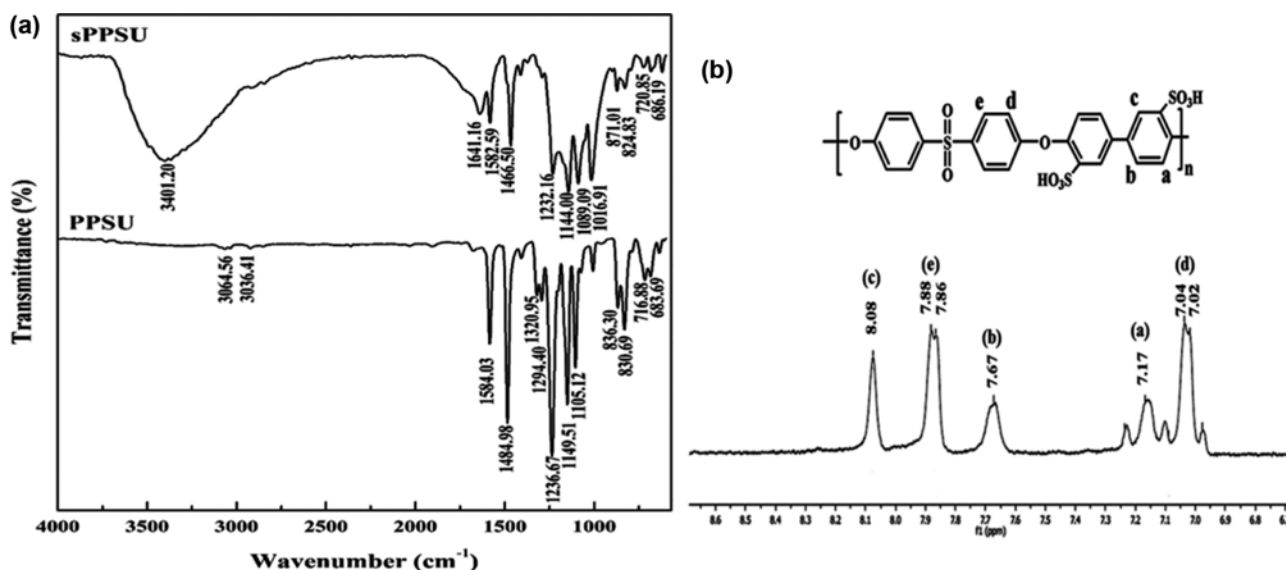$$\text{FRR}(\%) = \frac{J_{w2}}{J_{w1}} \times 100 \tag{7}$$

Fig. 1. (a) FTIR spectra of PPSU and sPPSU (b) ^{1}H NMR spectrum of sPPSU.

$$R_{rev}(\%) = \frac{(J_{w2} - J_p)}{J_{w1}} \times 100 \qquad (8)$$

$$R_{irr}(\%) = \left(\frac{J_{w1} - J_{w2}}{J_{w1}}\right) \times 100 \qquad (9)$$

RESULTS AND DISCUSSION

1. Polymer Characterization

The sPPSU was characterized by the ATR-FTIR and ^{1}H-NMR spectroscopy. The ATR-FTIR spectrum of sPPSU shows the presence of peak around 3,400 cm^{-1} and 1,640 cm^{-1} indicating the vibration of -OH from sulfonic acid groups interacting with molecular water (Fig. 1(a)). The peaks at 1,089 cm^{-1} are assigned to -SO$_3$H vibration, while 1,233 cm^{-1} and 1,016 cm^{-1} indicates SO$_3^-$ group in sPPSU [35]. The ^{1}H-NMR spectrum of sPPSU shows the characteristic peaks at chemical shift between 7-8.5 ppm (Fig. 1(b)). The presence of -SO$_3$H was validated by the peak at 8.08 ppm [24].

2. Membrane Characterization

The cross-sectional SEM images displayed the asymmetric nature of membranes with top dense layer and porous sub-layer with finger-like projections (Fig. 2). Increase in the concentration of sPPSU in the dope solution led to the strong H-bond interaction between the hydrophilic sulfonic group and water. This resulted in instantaneous demixing of solvent and non-solvent to give rise to elongated finger-like pores with increased porosity and pore size (Table 2). The variation in membrane thickness with gelation time, i.e., the time gap between the dipping of the casted plate into the coagulation bath and the emergence of opaque membrane film, is shown in Table 2. The gelation time for the membrane increased with the increase in sPPSU ratio, indicating the formation of thicker

Table 2. Membrane characteristics

Membrane code	Membrane thickness (μm)	Gelation time (s)	Pore radius (nm)	Porosity (%)
W 50	158	7	6.43	69.52
W 10	173	9	9.66	74.47
W 15	177	11	12.16	80.40
G 15	149	10	11.20	84.56
N 15	194	14	14.32	76.13
S 15	197	18	15.42	66.42

membranes. However, the concentration of sPPSU was limited to 5-15 wt% as the membrane showed poor film forming ability at higher concentration of sPPSU due to inhomogeneity in the blend above the 15 wt%.

The membrane with casting composition of PSF/sPPSU (85 : 15) was further studied for a better understanding of the effect of coagulation bath composition, as the membrane morphology is expected to change with the coagulation bath composition. The addition of NMP and NaCl to the coagulation bath suppressed the formation of macrovoid due to delayed liquid-liquid demixing [36], thereby resulting in a thick and dense membrane with low pore interconnectivity. The mass transfer of the solvent was observed to be slower for coagulation bath containing NaCl and NMP than the water as a coagulant. Moreover, the chemical potential of the coagulation bath decreased with the addition of NaCl due to the salt effect, thereby reducing the driving force for the film formation. However, the addition of GB to the coagulation bath displayed membranes with better morphology due to its high dipole moment and chemical potential [37]. GB in coagulation bath caused instanta-
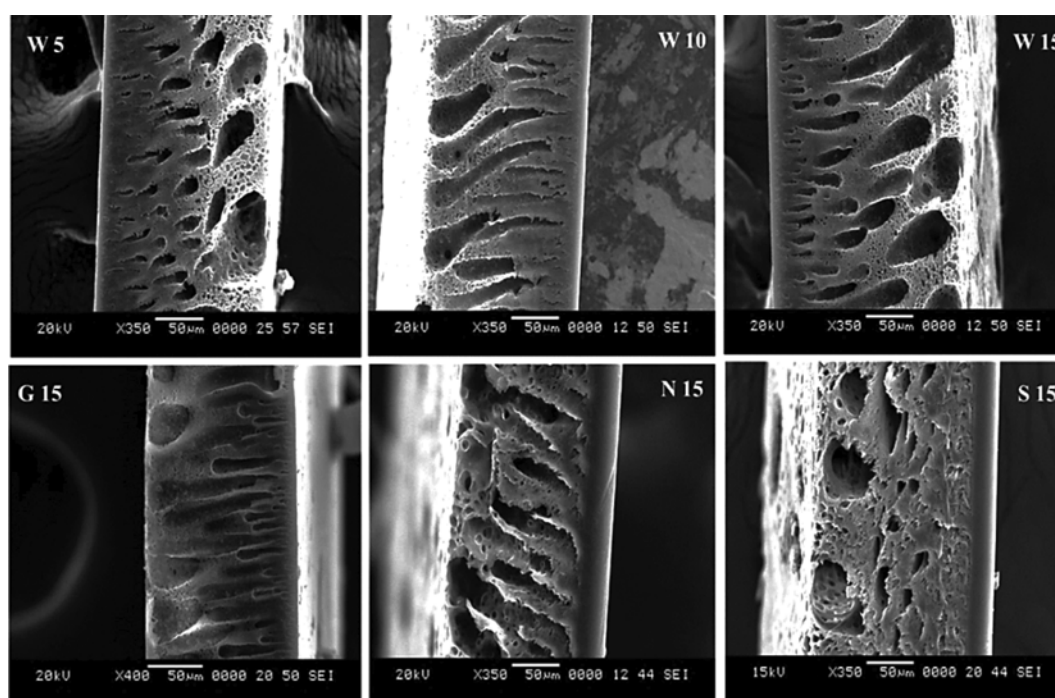

**Fig. 2. Cross-sectional images of prepared membranes.**

Table 3. Membrane properties

Membrane code	WCA (°)	Water uptake capacity (%)	Flux (Lm^{-2}h^{-1})			
			Pure water	Trypsin	Pepsin	BSA
W 5	65.42	60.68	125.30	73.74	51.449	23.27
W 10	62.68	66.47	149.98	87.60	72.36	39.27
W 15	56.04	71.56	190.70	108.52	94.25	60.84
G 15	55.88	75.46	203.36	131.48	101.73	65.65
N 15	56.50	68.19	153.77	80.78	68.44	42.15
S 15	57.08	57.25	103.44	62.49	42.33	22.35

neous demixing of the polymer-rich phase and polymer lean phase, resulting in a thin top layer and elongated finger-like projections. The variation in coagulation bath composition also affected the porosity of the membranes, which was in the following order: G 15> W 15>N 15>S 15. During the phase inversion, the instantaneous demixing with GB in coagulation bath resulted in porous membranes, while the slow mass transfer with coagulation bath containing NaCl and NMP caused dense membranes with lower porosity [38]. The variation in the pore size with the change in

coagulation bath composition is in the order: G 15<W 15<N 15< S 15, which is in accordance with the rate of demixing.

The hydrophilicity of the membranes was evaluated by the WCA and water uptake capacity measurement (Table 3). The decrease in WCA and increase in water uptake capacity can be observed by increasing the concentration of sPPSU. This is due to the migration of hydrophilic group to the surface of the membranes during the phase inversion, i.e., the hydroxyl group present in sulfonic acid has a strong affinity to water and forms H-bond with the water
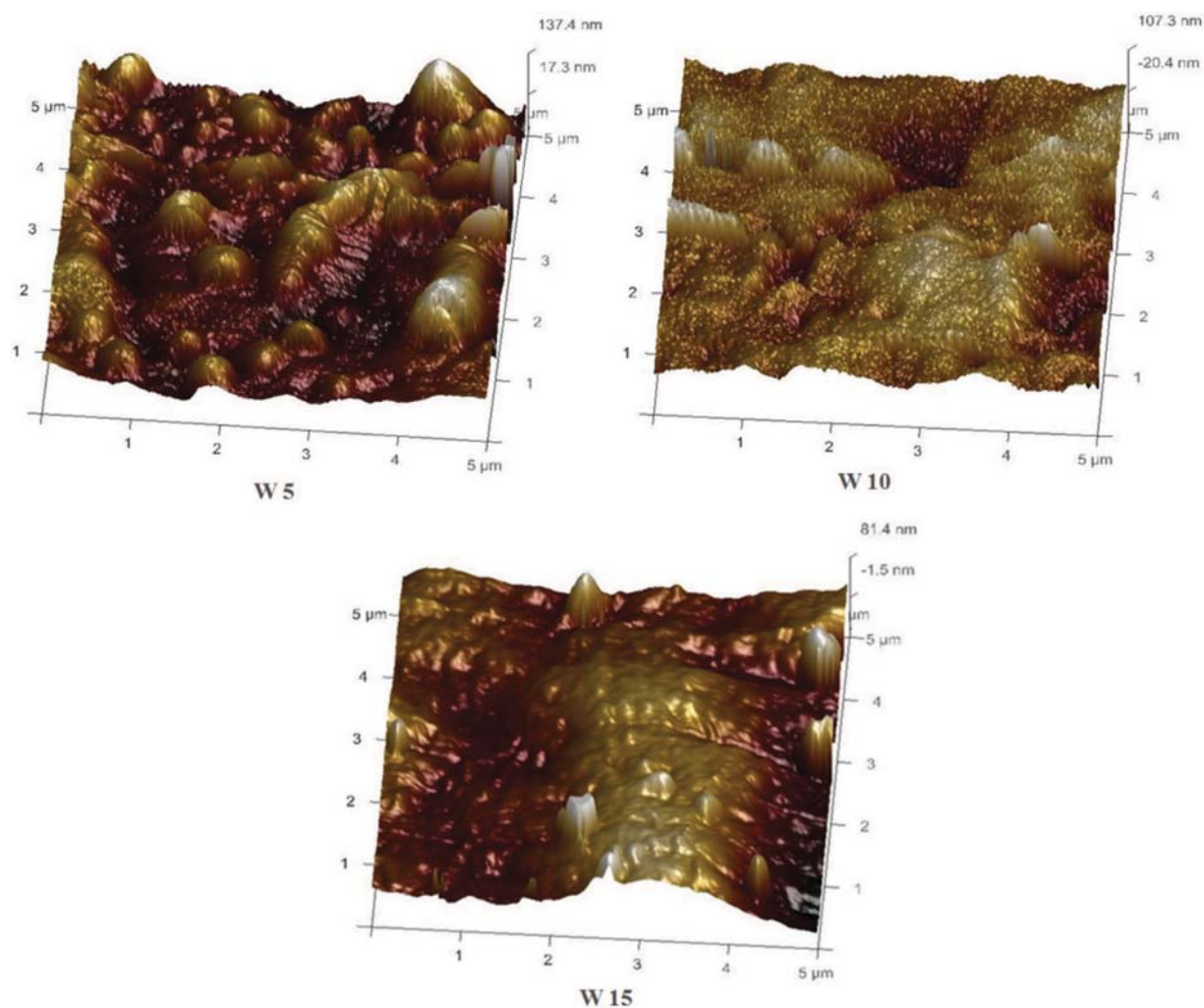
Fig. 3. 3D AFM images of prepared membranes.

molecule, resulting in the increase in surface wettability and hydrophilicity of the membranes. The hydrophilicity of the membranes was further increased with the increase in the concentration of sPPSU in the blend as the number of the sulfonic groups present on membrane surface increased. However, the coagulation bath did not bring any significant change in the WCA (Fig. S1 (supporting information)). However, there was a change in water uptake capacity of the membrane on varying the composition of coagulation bath. This is due to the morphological changes that have taken place in the membrane during the phase inversion. That is, the addition of GB to the coagulation bath improved the rate of demixing, thereby resulting in the membranes with elongated pores. The increased porosity of these membranes could enhance the ability of the membrane to retain water, in turn increasing the water uptake capacity. However, the water uptake capacity of the prepared membrane in the coagulation bath containing NaCl and NMP was observed to be lower due to their lower porosity and dense structure.

The surface roughness parameters of the membrane such as R_a and R_q were determined from AFM images. The membrane surface exhibited peaks (bright region) and valleys (dark region) when

Table 4. Surface roughness parameters of membranes

Membrane code	Roughness parameters	
	Ra (nm)	Rq (nm)
W 5	26.8	34.1
W 10	23.8	32.7
W 15	18.9	23.6

subjected to surface scan over an area of 5×5 μm under tapping mode [39]. It is clear from the images (Fig. 3) that the membrane showed fewer peaks and valleys with an increase in the concentration of sPPSU, hence displaying a smoother surface. The roughness of the membranes was further verified using the roughness parameters (Table 4), which were in the order of W 15<W 10<W 5 [40]. This decrease in surface roughness value indicates smoother surface, which is in correlation with the contact angle of membrane surface [41].

3. Filtration and Antifouling Study

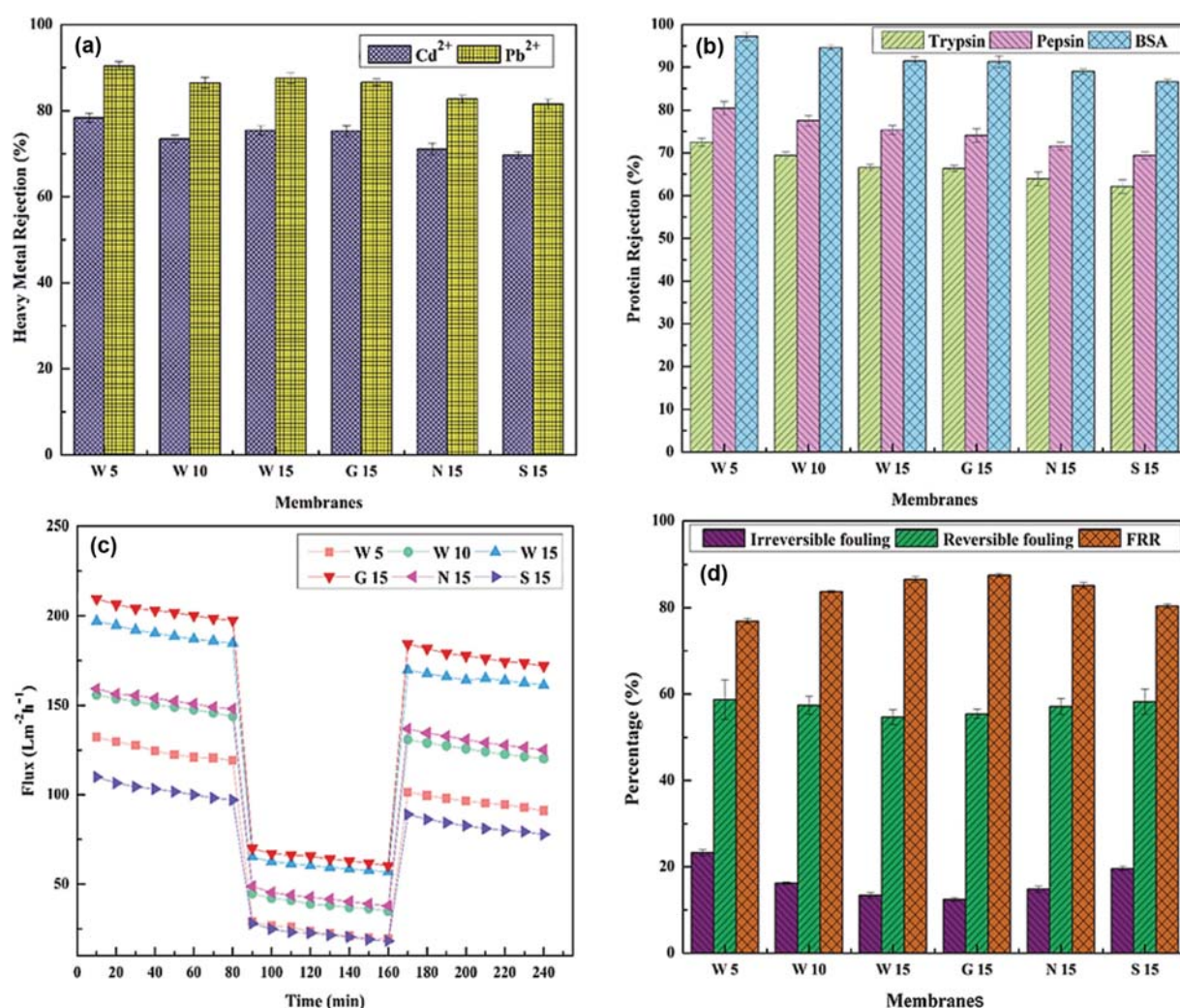The membrane permeability was estimated by measuring the

Fig. 4. (a) Heavy metal and (b) proteins rejection (c) flux vs. time for the membranes before and after passing BSA (d) fouling resistance by the membranes at 0.3 MPa TMP.

flux of water and protein solutions. The prepared membranes showed improved pure water and protein flux as the hydrophilicity, pore size, and porosity of the membranes increased with the increase in sPPSU concentration (Table 3). Further, the change in coagulation bath composition also affected the flux of the resulting membranes. The G 15 membrane displayed higher permeability due to greater porosity and water uptake capacity, as compared to W 15, which was thicker and denser. However, the S 15 and N 15 membrane showed lower flux due to their dense morphology and lower porosity.

The polymer enhanced UF (PEUF) was carried out by complexation of heavy metal ions with PEI [29]. The PEI-metal complex is formed as the metal interacts with the lone pairs of electrons present in the PEI, giving rise to macromolecules of larger size than the metal ions. Pb^{2+} showed greater rejection than Cd^{2+} due to the stronger binding of Pb^{2+} over Cd^{2+} in the PEI-metal complex, which was related to the electronegativity of metal ions [27,42,43]. The rejection of heavy metal ions declined as the pore size increased with increase in the composition of sPPSU in dope from 5 wt% to 10 wt%. The rejection eventually increased with the increase in the number of the negatively charged sulfonic group which dominated the increase of pore size. The larger pore size of the membrane prepared in a coagulation bath containing NMP and NaCl led to the lower rejection. The size exclusion and membrane charge density caused the overall rejection of 76-90% and 65-79% for Pb^{2+} and Cd^{2+} metal ions, respectively (Fig. 4(a)). The elemental mapping result demonstrates the adsorption of Pb^{2+} and Cd^{2+} on the membrane surface (Fig. 5).

The protein rejection was studied by measuring the amount of solute rejected on passing feed solution containing BSA (Mw~66.5 kDa), pepsin (Mw~34.5 kD) and trypsin (Mw~23.3 kDa). The superior protein flux and rejection could be attributed to the electrostatic repulsion of protein by the membrane surface, causing the reduced pore blockage [44]. The membranes showed increased protein rejection as the concentration of sPPSU in the dope increased. This is because of increased negative surface contributed by the sulfonic acid groups in sPPSU. The BSA demonstrated the least flux with the highest rejection, while trypsin showed the highest flux with least rejection, which is in accordance with the molecular weight of the protein. Trypsin with least molecular weight showed the highest flux with least rejection, while BSA, which has larger molecular weight, showed the highest rejection and least flux. The

sequence of protein rejection for the blend membranes with the change in coagulation bath follows: S 15<N 15<W 15<G 15 (Fig. 4(b)). The G15 membrane showed the highest flux for all the three protein samples with the maximum rejection of 66.3%, 74.0% and 91.2% for trypsin, pepsin, and BSA, respectively.

The antifouling behavior of the membranes was assessed by passing BSA solution through the prepared membranes. The flux decline was observed from Fig. 4(c), which is due to adsorption of BSA which blocked the pores on to the membrane surface. The order of fouling in the prepared blend membranes was W 15<W 10< W 5, which is in accordance with the surface hydrophilicity of the membranes. The extent of membrane fouling and reusability was studied by FRR, R_{rev} and R_{irr} fouling value (Fig. 4(d)). The increased FRR of the membrane was witnessed with the increase in the amount of sPPSU in the polymer, which indicates easy removal of adsorbed foulant. The weak interaction between the foulant and the membrane surface due to the formation of hydration layer makes it easier to wash away the foulant. The membrane with 15 wt% of sPPSU in blend showed least R_{irr} and R_{rev} of 13.43% and 54.67%, respectively. The presence of negatively charged -SO₃H group on the surface caused the electrostatic repulsion of the negatively charged protein foulant, hence lower adsorption of foulant on the membrane surface was observed [45]. The trend in membrane fouling was also justified by the AFM results, where the average roughness of the membrane was reduced with the increase in the ratio of the sPPSU present in the blend. It is well-established that a membrane with the lower surface roughness has better antifouling property. Consequently, the membrane with the rougher surface is undesirable as the uneven surface of the membrane encourage deposition of the foulant [46].

The effect of coagulation bath on the FRR was also studied, where the G 15 membrane showed slightly higher FRR than the S 15 and N 15. This was due to the hydrophilicity and the pore size of the membranes. The G 15 membranes with the highest hydrophilicity and lower pore size showed least R_{irr} as the membrane fouling due to clogging of the pore was reduced. While, S 15 and N 15 membranes, which possess lower hydrophilicity and higher pore size, showed lower FRR and increased R_{irr}.

CONCLUSIONS

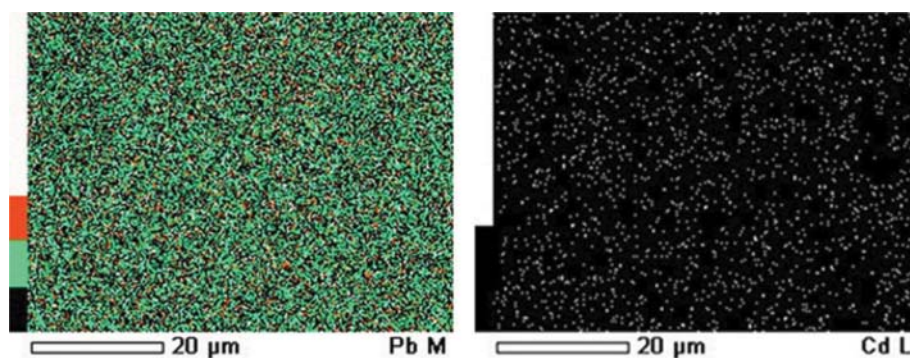The UF membranes prepared by blending PSF and sPPSU with

Fig. 5. Adsorption of Pb²⁺ and Cd²⁺ on the G 15 membrane.

different blend composition showed superior hydrophilicity and antifouling property. Incorporation of sPPSU into the dope solution gave rise to sulfonic acid groups on the surface of the membrane, which led to superior membrane performance. The blend membrane with 15 wt% concentration of sPPSU presented the best performance with PWF of 190.33 $Lm^{-2}h^{-1}$ and FRR of 86.56%. The lower fouling resistance of W 15 membrane demonstrated its reusability having R_{irr} and R_{rev} of 13.43% and 54.67%, respectively. The membrane morphology and performance varied on using different coagulation bath composition for phase inversion. The addition of GB to the coagulation bath resulted in a thinner membrane with higher porosity. The G 15 membrane showed the highest flux with 66.3%, 74.0% and 91.2% rejection of trypsin, pepsin, and BSA, respectively. However, the addition of NMP or NaCl to the coagulation bath affected the membrane performance adversely. The PEUF of Pb^{2+} and Cd^{2+} ions exhibited the rejection of 76-90% and 65-79%, respectively.

ACKNOWLEDGEMENTS

SUPPORTING INFORMATION

Additional information as noted in the text. This information is available via the Internet at http://www.springer.com/chemistry/journal/11814.

REFERENCES

1. R. Molinari, T. Poerio and P. Argurio, *Chemosphere*, **70**, 341 (2008).
2. S. Anbalagan, S. K. Ponnusamy, S. R. P. Selvam, A. Sankaranarayan and A. Dutta, *Korean J. Chem. Eng.*, **33**, 2716 (2016).
3. P. Kanagaraj, S. Neelakandan and A. Nagendran, *Korean J. Chem. Eng.*, **31**, 1057 (2014).
4. R. Ghosh, S. S. Silva and Z. Cui, *Biochem. Eng. J.*, **6**, 19 (2000).
5. P. G. Ingole and N. P. Ingole, *Korean J. Chem. Eng.*, **31**, 2109 (2014).
6. C. Mbareck, Q. T. Nguyen, O. T. Alaoui and D. Barillier, *J. Hazard. Mater.*, **171**, 93 (2009).
7. M. Kumar and J. Lawler, *Sep. Purif. Technol.*, **130**, 112 (2014).
8. A. K. Shukla, J. Alam, M. Alhoshan, L. A. Dass and M. Muthumareeswaran, *Scientific Reports*, **7**, 41976 (2017).
9. A. Rahimpour and S. Madaeni, *J. Membr. Sci.*, **305**, 299 (2007).
10. S. Nakao, H. Osada, H. Kurata, T. Tsuru and S. Kimura, *Desalination*, **70**, 191 (1988).
11. L. Q. Shen, Z. K. Xu, Z. M. Liu and Y. Y. Xu, *J. Membr. Sci.*, **218**, 279 (2003).
12. Y. Liu, X. Yue, S. Zhang, J. Ren, L. Yang, Q. Wang and G. Wang, *Sep. Purif. Technol.*, **98**, 298 (2012).
13. M. B. Thürmer, P. Poletto, M. Marcolin, J. Duarte and M. Zeni, *Mater. Res.*, **15**, 884 (2012).
14. S. Zhao, Z. Wang, J. Wang and S. Wang, *J. Membr. Sci.*, **469**, 316 (2014).
15. M. Shang, H. Matsuyama, M. Teramoto, D. R. Lloyd and N. Kubota, *Sep. Purif. Technol.*, **45**, 208 (2005).
16. E. Saljoughi, M. Amirilargani and T. Mohammadi, *J. Appl. Polym. Sci.*, **111**, 2537 (2009).
17. K. Y. Chun, S. H. Jang, H. S. Kim, Y. W. Kim, H. S. Han and Y. I. Joe, *J. Membr. Sci.*, **169**, 197 (2000).
18. S. Yang and Z. Liu, *J. Membr. Sci.*, **222**, 87 (2003).
19. M. Yam-Cervantes, J. Santiago-García, M. Loría-Bastarrachea, S. Duarte-Aranda, F. Alberto Ruiz-Treviño and M. Aguilar-Vega, *J. Appl. Polym. Sci.*, **134**, 4450 (2017).
20. S. Madaeni and A. Rahimpour, *Polymers for Advanced Technologies*, **16**, 717 (2005).
21. J. Xu, Y. Tang, Y. Wang, B. Shan, L. Yu and C. Gao, *J. Membr. Sci.*, **455**, 121 (2014).
22. C. Yao, R. Burford, A. Fane and C. Fell, *J. Membr. Sci.*, **38**, 113 (1988).
23. A. White and S. Jiang, *J. Phys. Chem. B*, **115**, 660 (2010).
24. M. Di Vona, E. Sgreccia, M. Tamilvanan, M. Khadhraoui, C. Chassigneux and P. Knauth, *J. Membr. Sci.*, **354**, 134 (2010).
25. M. Gil, X. Ji, X. Li, H. Na, J. E. Hampsey and Y. Lu, *J. Membr. Sci.*, **234**, 75 (2004).
26. S. Shenvi, A. Ismail and A. M. Isloor, *Ind. Eng. Chem. Res.*, **53**, 13820 (2014).
27. R. S. Hebbar, A. M. Isloor, K. Ananda and A. Ismail, *J. Mater. Chem. A*, **4**, 764 (2016).
28. I. K. Moideen, A. M. Isloor, A. Ismail, A. Obaid and H. K. Fun, *Desalin. Water Treat.*, **57**, 19810 (2015).
29. V. R. Pereira, A. M. Isloor, A. Al Ahmed and A. Ismail, *New J. Chem.*, **39**, 703 (2015).
30. R. S. Hebbar, A. M. Isloor, A. Ismail, S. J. Shilton, A. Obaid and H. K. Fun, *New J. Chem.*, **39**, 6141 (2015).
31. R. Kumar, A. M. Isloor, A. Ismail, S. A. Rashid and T. Matsuura, *RSC Adv.*, **3**, 7855 (2013).
32. M. Z. Yunos, Z. Harun, H. Basri and A. F. Ismail, *Desalination*, **333**, 36 (2014).
33. G. Lai, M. Yusob, W. Lau, R. J. Gohari, D. Emadzadeh, A. Ismail, P. Goh, A. Isloor and M. R. D. Arzhandi, *Sep. Purif. Technol.*, **178**, 113 (2017).
34. I. K. Moideen, A. M. Isloor, B. Garudachari and A. Ismail, *Desalin. Water Treat.*, **57**, 24788 (2016).
35. J. D. Kim, A. Donnadio, M. S. Jun and M. L. Di Vona, *Int. J. Hydrogen Energy*, **38**, 1517 (2013).
36. H. Strathmann and K. Kock, *Desalination*, **21**, 241 (1977).
37. K. Lutchmiah, L. Lauber, K. Roest, D. J. Harmsen, J. W. Post, L. C. Rietveld, J. B. van Lier and E. R. Cornelissen, *J. Membr. Sci.*, **460**, 82 (2014).
38. M. Buonomenna, P. Macchi, M. Davoli and E. Drioli, *Eur. Polym. J.*, **43**, 1557 (2007).
39. X. Cao, J. Ma, X. Shi and Z. Ren, *Appl. Surf. Sci.*, **253**, 2003 (2006).
40. P. Daraei, S. S. Madaeni, N. Ghaemi, E. Salehi, M. A. Khadivi, R. Moradian and B. Astinchap, *J. Membr. Sci.*, **415-416**, 250 (2012).
41. A. Razmjou, J. Mansouri and V. Chen, *J. Membr. Sci.*, **378**, 73 (2011).

42. T. Takagishi, S. Okuda, N. Kuroki and H. Kozuka, *J. Polym. Sci. Polym. Chem. Ed.*, **23**, 2109 (1985).

43. O. D. Kochkodan, V. M. Kochkodan and V. K. Sharma, *J. Environ. Sci. Health, Part A*, **53**, 33 (2017).

44. G. Liu, L. Zhang, S. Mao, S. Rohani, C. Ching and J. Lu, *Sep. Purif.* *Technol.*, **152**, 55 (2015).

45. L. P. Zhu, L. Xu, B. K. Zhu, Y. X. Feng and Y. Y. Xu, *J. Membr. Sci.*, **294**, 196 (2007).

46. A. Razmjou, J. Mansouri and V. Chen, *J. Membr. Sci.*, **378**, 73 (2011).

Supporting Information

Separation of heavy metal and protein from wastewater by sulfonated polyphenylsulfone ultrafiltration membrane process prepared by glycine betaine enriched coagulation bath

Irfana Moideen Kolangare*, Arun Mohan Isloor*,†, Asif Ali Qaiser**, Ahmed Fauzi Ismail***, and Mohd Sohaimi Abdullah***

*Membrane Technology Laboratory, Department of Chemistry, National Institute of Technology Karnataka, Surathkal, Mangalore-575 025, India
**Department of Polymer and Process Engineering, University of Engineering and Technology Lahore, 54890, Lahore, Pakistan
***Advanced Membrane Technology Research Center (AMTEC), Universiti Teknologi Malaysia, 81310 Skudai, Johor Bahru, Malaysia
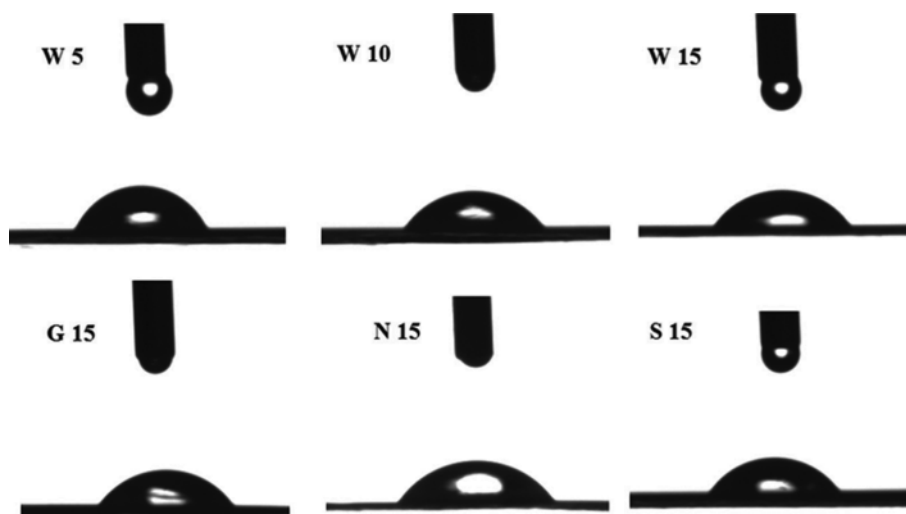
Fig. S1. Contact angle images of the prepared membranes.